A Generalized Approach to the Study of Voltage Inverters with Resonating Target Loads.

Marcel U. Agu, Ph.D. MNSE, MIEEE; Charles I. Odeh, Ph.D.; and Damian B.N. Nnadi, M.Eng.

Department of Electrical Engineering, University of Nigeria, Nsukka, Nigeria.

E-mail: nnadidamian@yahoo.com

ABSTRACT

This paper presents a generalized approach to the analysis and performance determination of inverters with target loads across which resonating AC voltages (usually very under-damped) are produced. This approach specifies the inverter circuit impedance components in per unit values of the impedance value at the resonant frequency of the impedance seen by the inverter output voltage or current. This per unitization method makes all relevant inverter impedance components and variables to be functions of the quality factor at the impedance resonant frequency. For any other inverter switching frequency between the upper and the lower limits about the resonant frequency, the normalized inverter circuit currents and voltages and the output transfer characteristics are easily determined as functions of only the circuit quality factor at resonance and the inverter operating frequency. It is demonstrated with varied topologies of inverters with target resonating loads that the generalized approach affords easy characterization and classification of these inverter types.

(Keywords: inverter, quality factor, resonant frequency)

INTRODUCTION

An inverter with a resonating target load produces resonating or ringing voltage across a specified target output load. An inverter resonating or ringing voltage or current has an expression that contains lightly damped or under-damped cosine and sine terms caused by the effect of inductors and capacitors intentionally introduced into the inverter circuit. Such a ringing load voltage and current afford the advantage of making the inverter active switch to totally or partially turn on and off at zero current and/or zero voltage. This resultant total or partial soft switching of the inverter active switches drastically reduces switching losses and makes possible inverter operation at high frequency. Operation at high frequency enormously reduces the size of capacitors and inductors necessary to achieve target load resonant or ringing action. Such inverter with resonant or ringing load is widely used for general purpose high frequency power supplies, high frequency dc to dc resonant link and induction heating.

In this paper, a generalized method is used to study the performance of such inverters with resonant ringing target loads. In the study, the relevant inverter per unit impedance components are specified at the resonant frequency of the impedance seen by the inverter output voltage or current and this specification method enables the inverter relevant impedances, voltages, currents and transfer gains to be expressed as functions of only the quality factor Q_n at the impedance resonance frequency f_n and inverter switching frequency . From the analysis results, the operational modes and characteristics of these inverter types can be generalized. The inverter topologies in this study are the single phase types with varied target ringing loads.

COMMON IMPEDANCE TYPES SEEN BY THE INVERTER OUTPUT CURRENT OR VOLTAGE

Figure 1 shows common load types seen by the inverter output voltage or current. The reactive components L, C_1 and C_2 are the inductor and the capacitances intentionally introduced to produce ringing or resonant voltage across the target impedance which is a resistance R_t in series with an inductance L_t. The values of L_t and R_t depend on the nature of the target load.

In many applications, L_t is negligible and R_t models the resistance in which useful power is expended. In many other applications, such as the induction heating of ferromagnetic materials, L_t is appreciable and the target impedance is L_t in series with R_t.

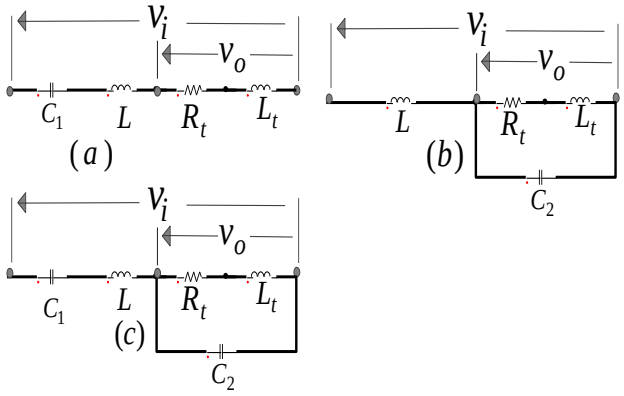

Figure 1: Common Impedance Configuration Types Seen by the Inverter Output Voltage or Current in Inverters with Ringing Target Load (R_t in series with L_t).

Specifying the Per Unit Impedance Components with L_t Negligible

With L_t negligible, the equivalent per unit components of the impedance configuration of figure 1 at the respective resonant frequencies of the impedance configuration are as shown in figure 2 where each impedance configuration is classified as series connected, parallel connected and series-parallel connected according to the position of R_t relative to the position of the resonant capacitors C_1 in Figures 2a and 2b and C_1 and C_2 in Figure 2c The respective quality factors Q_n at the resonant frequencies of the respective impedance configurations, the base impedance Z_b and the resonant frequency $\omega_n = 2\pi f_n$ for each impedance configuration are expressed as follows:

For Figure 2a:

$$Qn = \frac{\omega_n L}{R_t}, \qquad Z_b = R_t = 1\ p.u., \qquad \omega_n = 2\pi f_n = \frac{1}{\sqrt{LC_1}} \tag{1}$$

For Figures 2b and 2c:

$$Qn = \frac{1}{\omega_n C_1 R_t}, \qquad Z_b = \frac{L}{R_t C_1} = 1 p.u., \qquad \omega_n^2 = \frac{1}{L C_1} - \frac{1}{R_t^2 C_1^2} \tag{2}$$

The per unit values of each impedance configuration of Figure 2 are obtained by the simultaneous solution of the three equations for each configuration. For each impedance configuration, the per unit impedance components result in the per unit value of the resonant frequency being unity. It should be noted in Figure 2c that the relation between capacitors C_1 and C_2 is:

$$C_1 = kC_2 \tag{3}$$

where k is a constant.

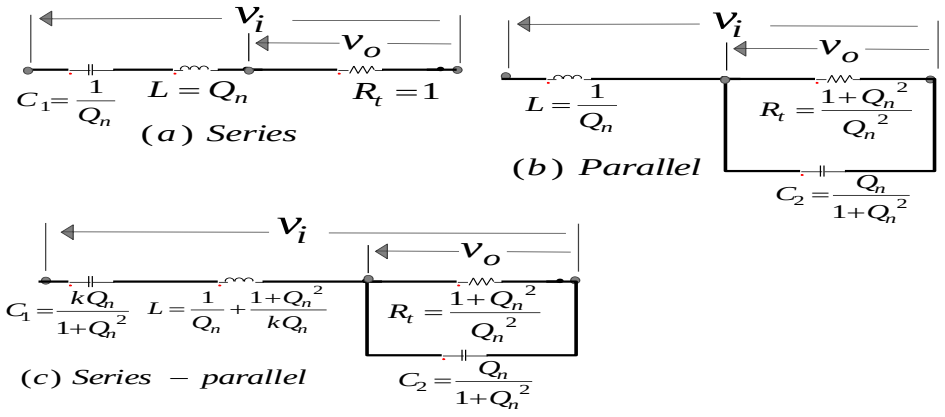

Figure 2: Per Unit Components of the Impedance Configurations of Figure 1 (with L_t negligible) at the Respective Resonant Frequencies of the Impedance Configurations.

Also it should be noted that the chosen resonant frequency of Figure 2c is the same as that of Figure 2b and that the reactance of the series inductance L is adjusted to cancel the reactance of the introduced capacitance C_1 at the resonant frequency ω_n.

The Voltage Gain $\frac{v_o}{v_i}$

For each impedance configuration, the voltage gain $\frac{v_o}{v_i}$ (the ratio of the input voltage to the target load voltage) at the per unit frequency ω p.u. of the applied input voltage can be obtained. As an illustration, the voltage gains for Figures 2a and 2b are:

$$\frac{v_o}{v_i} = \frac{1}{(1+Q_n{}^2(\omega - 1/\omega)^2)^{\frac{1}{2}}}$$

For Figure 2a **(4)**

$$\frac{v_o}{v_i} = \sqrt{\frac{(1+\frac{\omega^2}{Q_n{}^2})}{1+\frac{\omega^2}{Q_n{}^2}(\frac{\omega^2-1}{1+Q_n{}^2})}}$$

For Figures 2b & 2c **(5)**

Figure 3 shows the plot of the voltage gain against the per unit frequency with the quality factor as parameter for the three impedance configurations. The plots show that the target load receives voltage much boosted far above the input voltage (especially at the resonant frequency ω_n for Figures 2b and 2c) while that of the series RLC load of Figure 2a has a target voltage whose maximum value is unity at the resonant frequency ω_n.

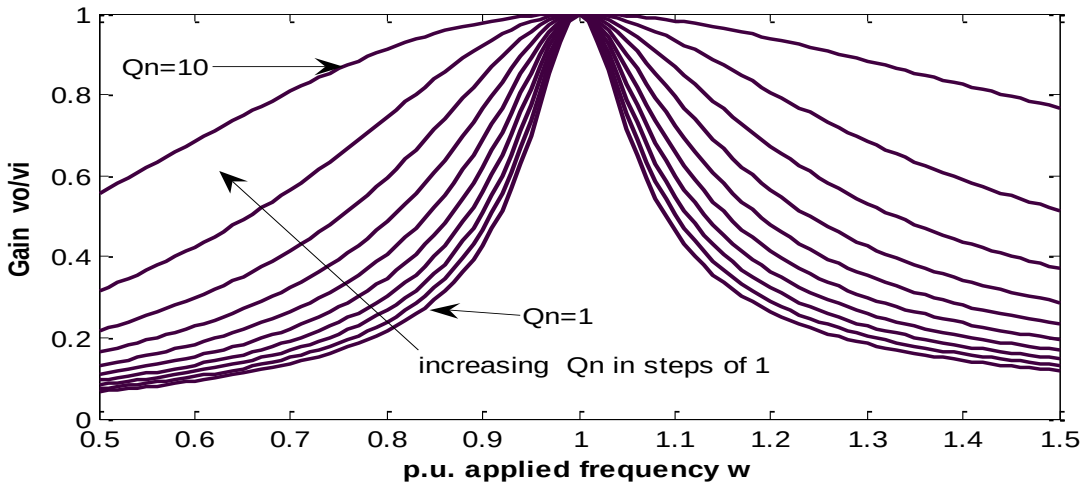

Figure 3a: Output/Input Voltage Gain v_o/v_i Against P.U. Frequency (ω) of the Series Loaded Circuit of Figure 2a.

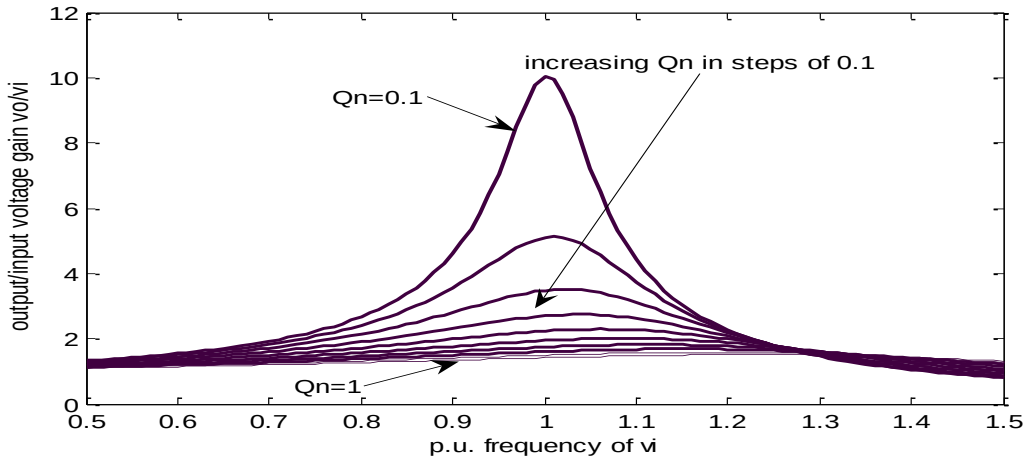

Figure 3b: Output/Input Voltage Gain v_o/v_i against P.U. Frequency (ω) of the Parallel Loaded Circuit of Figure 2b.

Specifying the Per unit Impedance Component with L_t not Negligible

With L_t not negligible, Equations 1 and 2 are modified as:

For Figure 1a:

$$Qn = \frac{\omega_n (L + L_t)}{R_t}, \qquad Z_b = R_t = 1 p.u., \qquad \omega_n = 2\pi f_n = \frac{1}{\sqrt{(L + L_t) C_1}} \qquad \textbf{(6)}$$

For Figures 1b and 1c:

$$Qn = \frac{\omega_n L_t}{R_t}, \qquad Z_b = \frac{L_t}{R_t C_1} = 1 p.u., \qquad {\omega_n}^2 = \frac{1}{L_t C_1} - \frac{{L_t}^2}{{R_t}^2} \qquad \textbf{(7)}$$

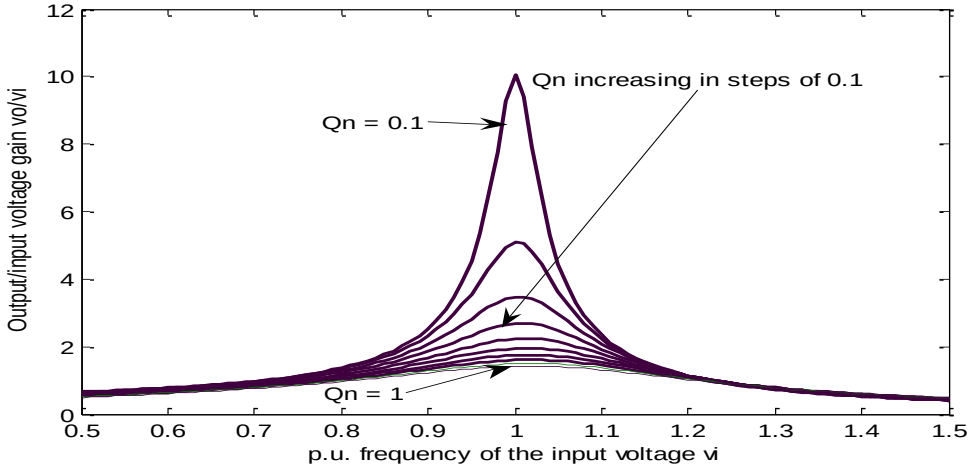

Figure 3c: Output/input Voltage Gain v_o/v_i against P.U. Frequency (ω) of the Parallel Loaded Circuit of Figure 2c.

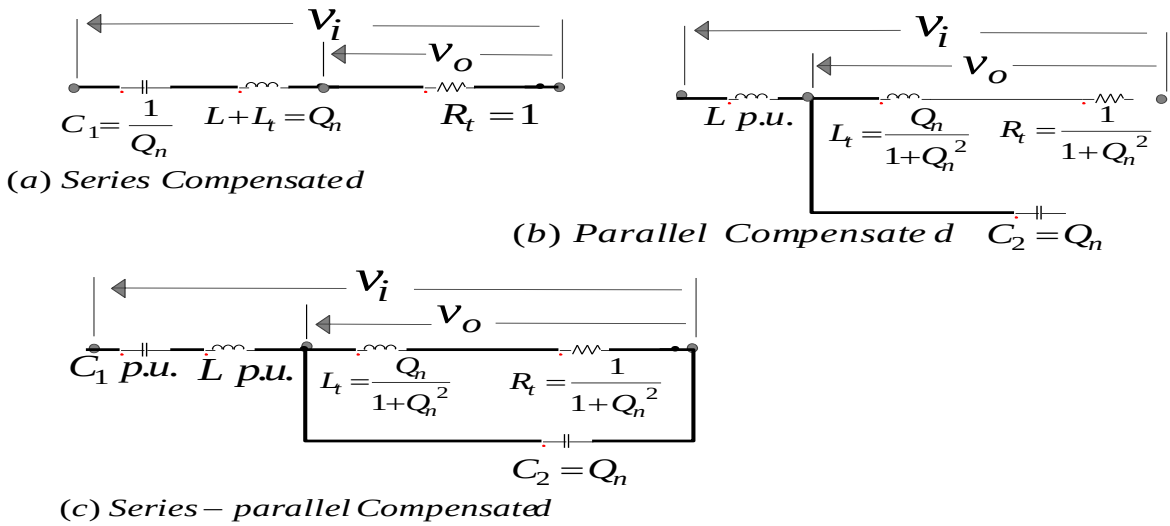

Figure 4: Per Unit Components of the Impedance Configurations of Figure 1 (with L_t not negligible) at the Respective Resonant Frequencies of the Impedance Configurations.

The series components (L in Figure 1b and L and C_1 in Figure 1c) are specified as convenient per unit values to control the peak and the rate of rise of the inverter output current. Simultaneous solution of each of the three Equations of 6 and 7 give the values of the impedance components as shown in Figures 4a - 4c.

THE INVERTER CIRCUITS WITH THE TARGET RINGING LOADS OF FIGURE 2

The inverter configurations with the per unit impedance configurations of Figure 2 are of two main types namely; inverters with bidirectional active switches and inverters with unidirectional switches.

Inverters With Unidirectional Switches

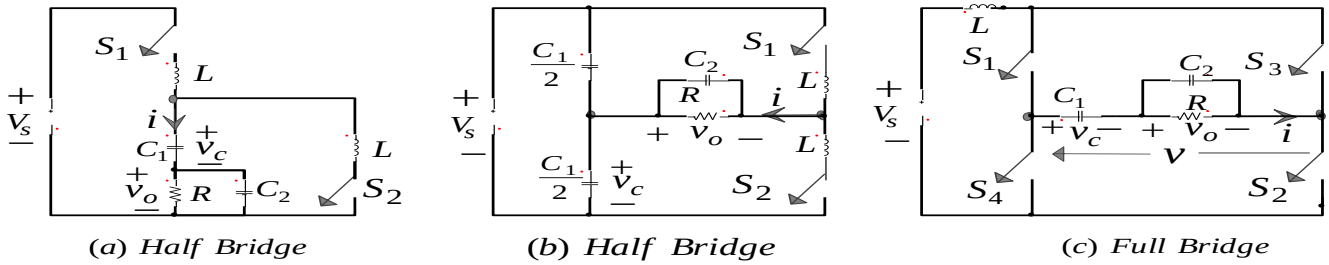

Figure 5: Forms of Resonant Inverters with Unidirectional Active Switches.

Table 1: The Per Unit Values of the Impedance Components of the Inverter Circuits of Figure 5.

Inverter Configuration	Per unit impedance components as functions of Q_n		
	Series Loaded	**Parallel Loaded**	**Series-Parallel loaded**
Figure 5a (half bridge) and Figure 5c (full bridge)	$L = Q_n$ $C_1 = \frac{1}{Q_n}$ $C_2 = 0 (open\ circuit)$ $R_t = 1$	$L = \frac{1}{Q_n}$ $C_1 = \infty (short\ circuit)$ $C_2 = \frac{Q_n}{1+{Q_n}^2}$ $Rt = \frac{1+{Q_n}^2}{{Q_n}^2}$	$L = \frac{1}{Q_n} + \frac{1+{Q_n}^2}{kQ_n}$ $C_1 = \frac{kQ_n}{1+{Q_n}^2}$ $C_2 = \frac{Q_n}{1+{Q_n}^2}$ $R_t = \frac{1+{Q_n}^2}{{Q_n}^2}$
Figure 5b (half bridge)	$L = Q_n$ $C_1 = \frac{1}{Q_n}$ $C_2 = 0 (open\ circuit)$ $R_t = 1$	Not Feasible	$L = \frac{1}{Q_n} + \frac{1+{Q_n}^2}{kQ_n}$ $C_1 = \frac{kQ_n}{1+{Q_n}^2}$ $C_2 = \frac{Q_n}{1+{Q_n}^2}$ $R_t = \frac{1+{Q_n}^2}{{Q_n}^2}$

Figures 5a – 5c show the inverter circuits with unidirectional active switches and the generalized ringing circuit configuration. Table 1 shows the per unit values of the impedance components of the inverter circuits of Figure 5 for the three load impedance configurations of Figure 2.

Using the Series Loaded Inverter of Figure 5a as an Illustration

With the series loaded inverter of Figure 5a as an illustration, the load current flows through a series combination of L, C_1 and R_t in each half cycle for each inverter of Figure 5. This inverter output current i can be shown to be given as:

$$i = I_{mo} e^{-\xi t} \sin \omega_r t, \qquad 0 < t < \frac{\pi}{\omega_r} \tag{8a}$$

$$i = 0, \qquad \frac{\pi}{\omega_r} < t < \frac{\pi}{\omega} \tag{8b}$$

$$i = I_{mo} e^{-\xi (t - \frac{\pi}{\omega})} \sin \omega_r (t - \frac{\pi}{\omega}), \qquad \frac{\pi}{\omega} < t < \frac{\pi}{\omega} + \frac{\pi}{\omega_r} \tag{8c}$$

where

$$I_{mo} = \frac{V_s}{\omega_r L (1 - e^{-\frac{\pi \xi}{\omega_r}})}$$

for Figures 5a and 5b **(9)**

and ω is the inverter switching or operating frequency.

I_{mo} for Figure 5c is double that of Figures 5a and 5b. The ringing frequency ω_r and the damping ratio ξ are:

$$\xi = \frac{1}{2 Q_n} \tag{10}$$

$$\omega_r = \sqrt{1 - \frac{1}{4Q_n}} \qquad \textbf{(11)}$$

The active switch peak voltage v_{sp} and the resonant capacitor peak voltage v_{cp} can be shown to be given by:

$$v_{sp} = V_s\left(1 + \frac{e^{-\frac{\xi(\pi - 2\psi)}{\omega_r}}}{1 - e^{-\frac{\pi\xi}{\omega_r}}}\right)$$

For Figures 5a and 5b **(12a)**

$$v_{cp} = \frac{V_s}{1 - e^{-\frac{\pi\xi}{\omega_r}}}$$

For Figures 5a and 5b **(12b)**

$$v_{sp} = V_s\left(1 + \frac{2e^{-\frac{\xi(\pi - 2\psi)}{\omega_r}}}{1 - e^{-\frac{\pi\xi}{\omega_r}}}\right)$$

For Figure 5c **(13a)**

$$v_{cp} = V_s\left(\frac{1 + e^{-\frac{\pi\xi}{\omega_r}}}{1 - e^{-\frac{\pi\xi}{\omega_r}}}\right)$$

For figure 5c **(13b)**

where,

$$\psi = \tan^{-1}\frac{\xi}{\omega_r} \qquad \textbf{(13c)}$$

Similar analysis as carried out for the inverters of figure 5b to 5c with series loads can also be carried out for the inverters when parallel or series parallel loads are used. For the parallel loading, it can be shown that the ringing frequency, $\omega_r = 2\pi f_r$, and the damping ratio ξ are:

$$\xi = \frac{Q_n}{2(Q_n + 1)} \qquad \textbf{(14)}$$

$$\omega_r = \sqrt{1 + Qn^2 - \frac{1}{4(Q_n{}^2 + 1)}} = 2\pi f_r \qquad \textbf{(15)}$$

Generally, for $Q_n >> 1$ for the series loaded inverter and $Q_n << 1$ for the parallel and series-parallel loaded inverter, the ringing frequency $\omega_r = 2\pi f_r$ and the resonant frequency ω_n are related as:

$$\omega_r \approx \omega_n \qquad \textbf{(16)}$$

Alternatively, the damping ratio and the ringing frequency can easily be determined for all inverter loading types by solving for the roots of the characteristic equation of the voltage gain $\frac{v_o}{v_i}$ expressed in Laplace domain.

The Limitation of Resonant Inverters with Unidirectional Switches

The limitations of each inverter circuit of Figure 5, irrespective of its simplicity, are:

(a) Since a switch current must be zero before the turning off of the switch and turning on the next active switch, the maximum inverter operating frequency is half the design ringing frequency and this makes the inverter output current to be always discontinuous.

(b) Control of the power delivered to R_t is only by frequency modulation.

(c) The active switch voltage is relatively very high and increases with decrease in the damping ratio ξ.

Illustrative Circuit Waveforms

Figure 6 shows the per cycle inverter output current, i, the target load voltage v_o, the resonant capacitor C_1 voltage v_{c1} and the active switch S_1

voltage v_{s1} for the circuit of figure 5a with the voltages in per unit of the inverter dc input voltage. The high gain v_o/V_s of the parallel and series parallel connections relative to the series connected load confirm the gain plots of Figure 3.

Resonant Inverters with Bi-Directional Active Switches

Figure 7(a-b) shows the half bridge and the full bridge inverters with bidirectional active switches and the generalized ringing load of the series parallel type. The inverter loading can be altered to any of the loading types shown in Table 1.

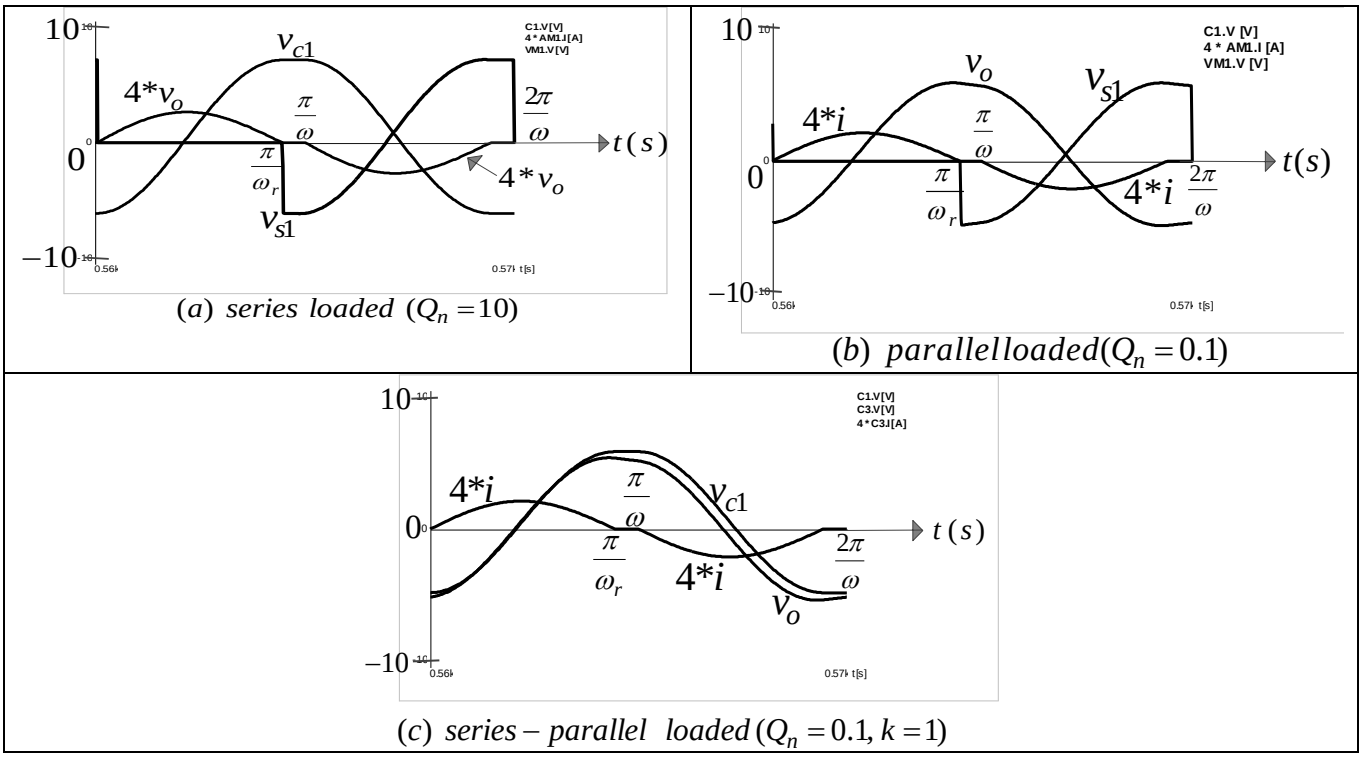

Figure 6: Illustrative Circuit Waveforms of the Inverter of Figure 5a with Resonant Series, Parallel and Series-Parallel Connected Output Impedances.

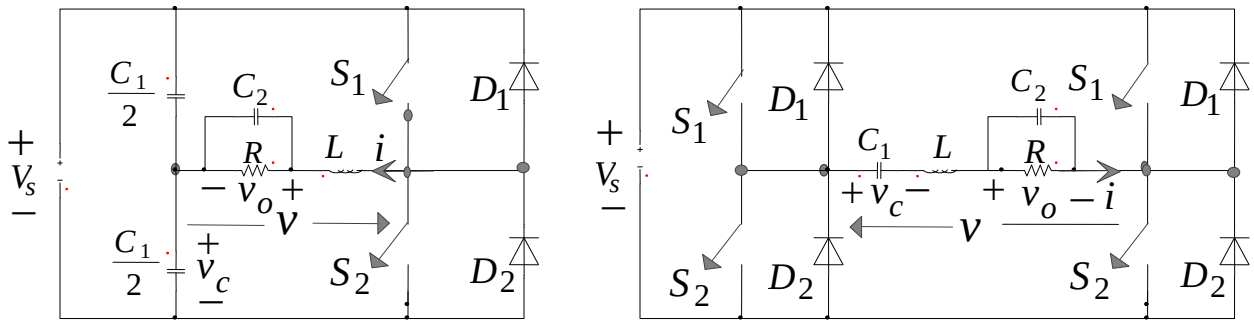

Figure 7: Forms of Resonant Inverters with Bidirectional Active Switches.

Unlike in the case of the inverters with unidirectional switches only, in the case of these inverters with bidirectional switches the inverter output current i can be continuous or discontinuous because of the presence of the anti-parallel diodes to conduct reverse inverter output current, i .

Discontinuous Inverter Output Current ($\frac{T}{2} > T_r$ or $\frac{f_r}{2} > f$).

In the frequency range $\frac{f_r}{2} > f$ for all inverter topologies and load types , the inverter output current i is discontinuous and in a given half cycle of period $\frac{T}{2}$ flows through the active switches for an interval $\frac{T_r}{2}$ and then through the anti-parallel diodes for the next $\frac{T_r}{2}$ interval.

Case with the Series Loaded Inverter

Under discontinuous current mode for the series loaded half bridge inverter of Figure 7a, the inverter output current i has the form given in (8) but with I_{mo} given as:

$$I_{mo} = \frac{V_s}{\omega_r L(1 + e^{-2\pi\xi/\omega_r})} \quad \textbf{(17a)}$$

While the peak resonant capacitor voltage V_{cp} is:

$$V_{cp} = V_s\left[1 + \frac{e^{-2\pi\xi/\omega_r}}{1 + e^{-2\pi\xi/\omega_r}}\right] \quad \textbf{(17b)}$$

For the series loaded form of the full bridge inverter of Figure 7b, I_{mo} is double of that given in (17a), while the increase of V_{cp} above the source voltage V_s is double of that given in (17b).

Figure 8 shows illustrative circuit waveforms ((a) Q_n = 10 and (b) Q_n = 0.1) for discontinuous half bridge inverter output current operation under the two loading conditions of Table 1. In terms of voltage gain, $\frac{v_o}{v_i}$ Figure 8b for the series-parallel loaded inverter configuration shows superior performance over Figure 8a for the series loaded inverter.

Continuous Inverter Output Current Operation ($\frac{T}{2} \le T_r$ or $\frac{f_r}{2} \le f$).

In the frequency range $\frac{f_r}{2} \le f$, the inverter output current is continuous for all inverter loading types and configurations. The general expression of the inverter output current in the positive half cycle is

$$i = K_1(\xi, \omega_r)V_s e^{-\xi t}\sin\omega_r t + K_2(\xi, \omega_r)I_{in}e^{-\xi t}\cos\omega_r t \quad \textbf{(18)}$$

where I_{in} is the value of the output current at the instant of changing the active switch conducting pattern by turning on the next incoming active switch(es) while K_1 and K_2 are functions of the ringing frequency ω_r and the damping ratio ξ .
The obvious merits of the resonant converters with bi-directional switches at continuous current conduction are:

a) Reduced active voltage stress as the peak active voltage is damped to the value of the source voltage.

b) Both frequency and pulse width modulation methods can be used to control the targeted ringing load voltage v_o .

c) Operation at the resonant frequency ω_n for maximum power transfer to the targeted load is easily possible.

The partial soft switching that occurs at $\frac{f_r}{2} < f$ is easily made completely soft switching by the introduction of small inductor at the inverter input for $\frac{f_r}{2} < f < f_r$ and small snubber capacitors across the active switches for $f > f_r$ As an illustration, Figure 9a-b show continuous load current operation of the parallel loaded full bridge inverter at $\frac{f_r}{2} < f < f_r$ and $\frac{f_r}{2} > f$.

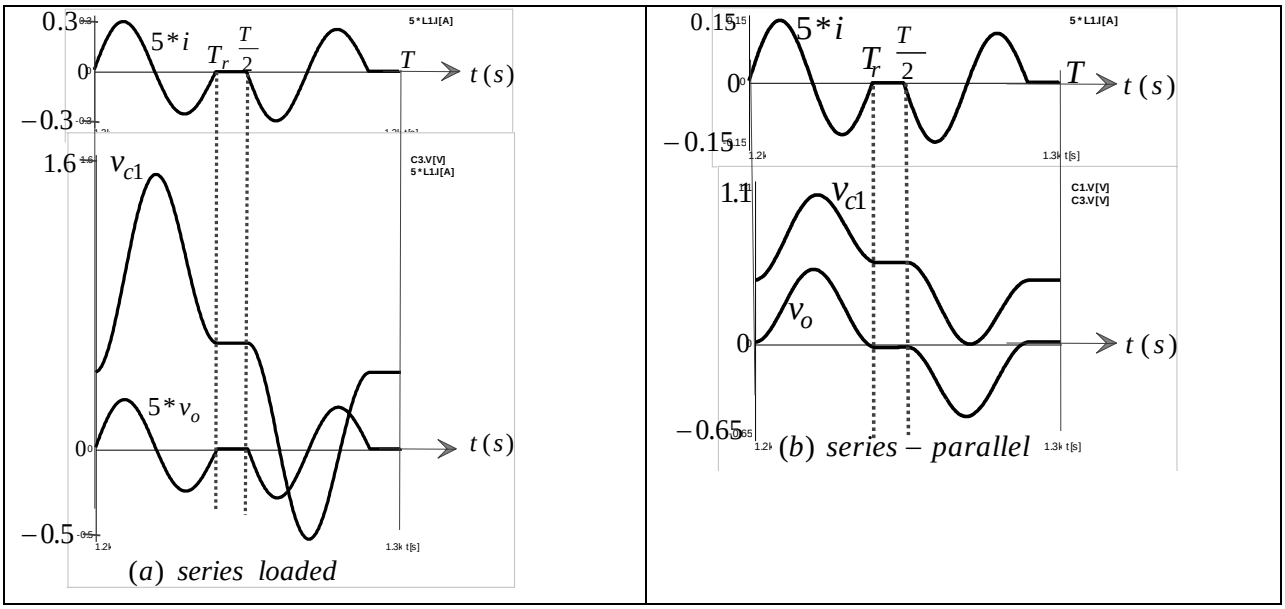

Figure 8: Discontinuous Inverter Output Current Operation of the Half Bridge Inverter Circuit of Figure 7a.

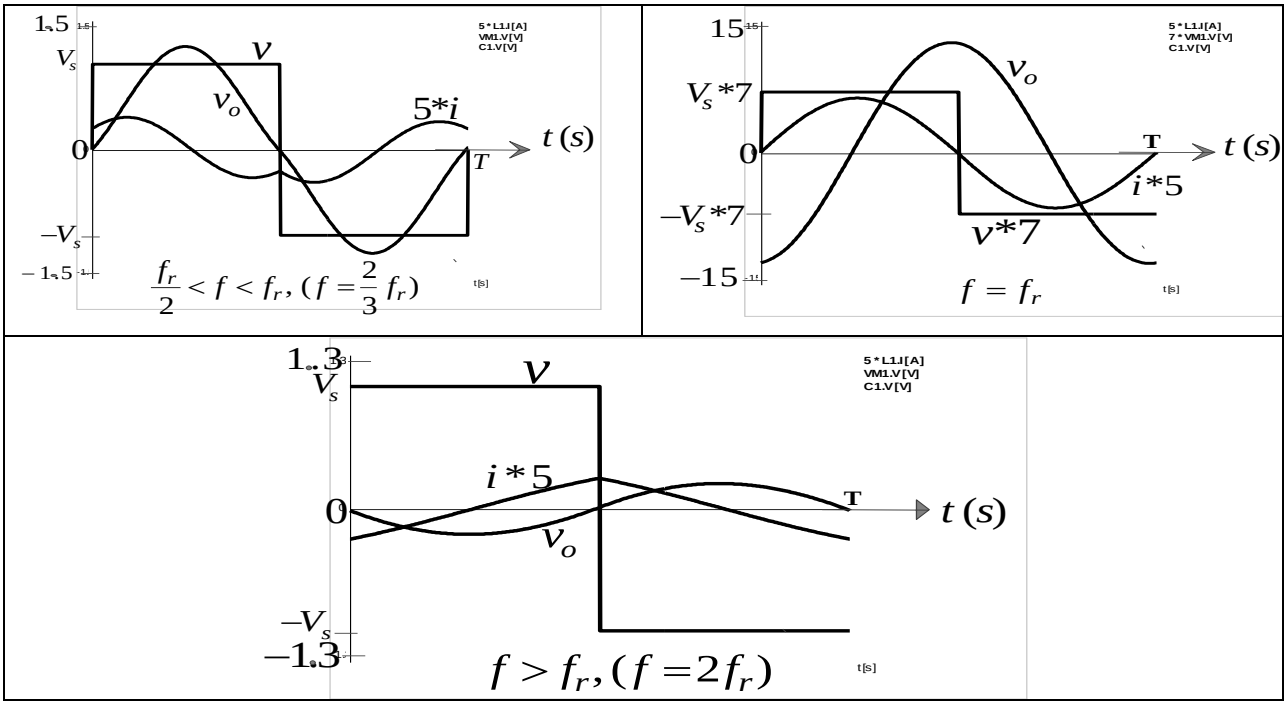

Figure 9: Continuous Inverter Output Current Operation of the Series-Parallel Loaded Full Bridge Inverter Circuit of Figure 7b (Q_n = 0.1).

FULL BRIDGE INVERTER WITH OUTPUT CAPACITOR COMPENSATED R_tL_t TARGET LOADS

The full bridge inverter is the most appropriate to use for the compensated R_tL_t target loads. Figure 10 shows a full bridge inverter circuit with the generalized compensated R_tL_t target load of Figure 4c.

For operation at the tank load resonant frequency $\left(\omega_n = \sqrt{\frac{1}{L_t C_2} - \left(\frac{L_t}{R_t}\right)^2} \right)$, the per unit impedances are as given in fig 4. For fig 4c output impedance, the reactances of C_1 and L are chosen to be equal at the centre frequency of operation. As R_t and L_t varies, both inverter switching frequency and inverter output pulse-width can be varied to maximize input/output power transfer to the target load as well as maintain the target load voltage or power at a desired value.

Figure 11 shows illustrative waveforms of the operation of the inverter circuit of Figure 10 when both the inverter switching frequency and the output voltage pulse-width are adjusted so that:

(a) the fundamental inverter output current i is in phase with the target load voltage v_o.

(b) The inverter output current i is in phase with the inverter output voltage v.

Both methods are alternate techniques for high circuit performance.

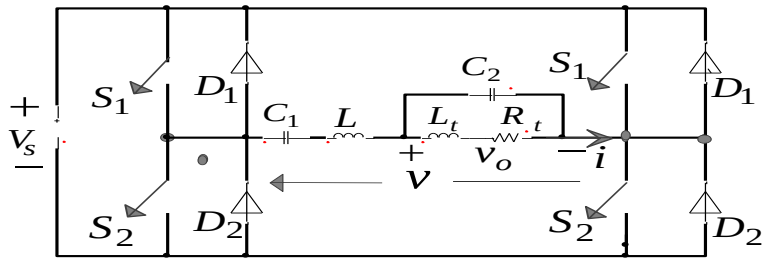

Figure 10: Full Bridge Inverter with L_t- R_t Capacitor Compensated Load.

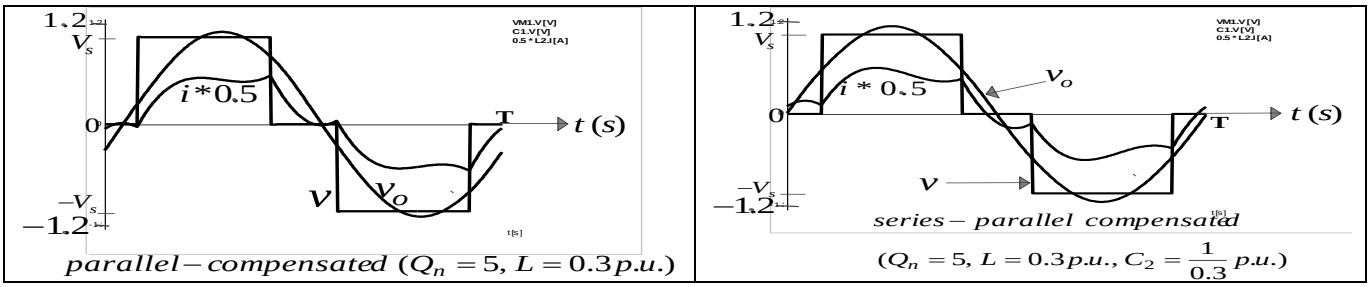

Figure 11: Circuit Waveforms of the Inverter of Figure 10 with Capacitor Compensated R_t-L_t Load and Inverter Operation at Tank Load Resonant Frequency f_n.

CONCLUSION

In this paper, a general method of per unitization of the parameters and variables of voltage fed inverters with target ringing loads has been presented. In the per unitization method, the circuit parameters and variables are reduced to be functions of only the circuit quality factor Q_n and the inverter operating frequency (f). This makes easy the determination and classification of the inverter circuit performance. The range of target ringing loads considered in the paper covers wide range of applications in high frequency resonant dc to dc links and induction heating. With significant improvement in power semiconductor devices (such as insulated Gate Bipolar Transistor, the MOSFET, etc), the work introduces improved and viable methods of supplying ringing target loads in power supply and induction heating applications.

REFERENCES

1. Dewan, S.B. and A. Straughen. 1984. *Power Semiconductor Circuits*. John Wiley and Sons: New York, NY.

2. Moo, C.S., Y.C. Chuang, and C.R. Lee. 1994. "A New Power Correction Circuit for Fluorescent Ballasts with Series Resonant Inverter". *Proceedings of IEEE APEC'94*. 441-449.

3. Bhat, A.K.S. and S.B. Dewan. 1984. "A Generalized Approach for the Steady State Analysis of Resonant Inverter". IEEE Industry Applications Society Conference. 640-647.

4. Rashid, M.H. 1993. Power Electronics Circuits, Devices and Applications". Prentice-Hall: Englewood Cliffs, NJ.

5. Sen, P.C. 2004. *Modern Power Electronics*", S. Chand and Company Ltd.: New Delhi, India.

ABOUT THE AUTHORS

Marcel U. Agu was born in Ohebe Dim, Nigeria, in 1947. He received his B.Sc. degree from the University of Nigeria, Nsukka in 1974 and his M.A.Sc. and Ph.D. degrees in Power Electronics from the University of Toronto, Canada in 1978 and 1982, respectively. He is currently a Professor of Electrical Engineering in the Electrical Engineering Department of the University of Nigeria, Nsukka. He has been engaged in research and teaching in the areas of power electronics and drive systems.

Charles I. Odeh was born in Adani, Nigeria. in 1976. He received B.Eng. and M.Eng. degrees from the University of Nigeria, Nsukka in 2002 and 2006, respectively. He earned his Ph.D. degree in Power Electronics at the University of Nigeria, Nsukka in 2010. His research interests are in power electronics and machine drives.

Damian B.N. Nnadi was born in Obollo-Afor, Enugu State Nigeria in 1973. His B.Eng. and M.Eng. degrees were received from Enugu State University of Science and Technology (ESUT) in 1999 and 2004 respectively. He is currently pursuing his Ph.D. degree in Power Electronics at the University of Nigeria, Nsukka Research interest is in renewable energy and power electronics

SUGGESTED CITATION

Agu, M.U., C.I. Odeh, and D.B.N. Nnadi. 2011. "A Generalized Approach to the Study of Voltage Inverters with Resonating Target Loads". *Pacific Journal of Science and Technology*. 12(2):8-19.

Pacific Journal of Science and Technology